*Mathematical Biosciences and Engineering*

http://www.aimspress.com/journal/mbe

MBE, 22(8): 1931–1955.
DOI: 10.3934/mbe.2025070
Received: 25 February 2025
Revised: 15 April 2025
Accepted: 25 April 2025
Published: 19 June 2025

*Research article*

# Modelling behavioural interactions in infection disclosure during an outbreak: An evolutionary game theory approach

**Pranav Verma†, Viney Kumar† and Samit Bhattacharyya***

Disease Modelling Lab, Department of Mathematics, School of Natural Sciences, Shiv Nadar Institution of Eminence, Gautam Buddh Nagar 201314, India

† These authors contributed equally to this work.

* **Correspondence:** Email: samit.b@snu.edu.in.

## Supplementary

### S1. Preliminaries

Let $f$ be a real-valued differentiable function. The $n^{th}$ Cauchy repeated integral formula gives an expression for compressing $n \in \mathbb{N}$ repeated integrals of $f$ into a single antiderivative on an interval with base point $a$, which is given by [1]:

$$ {}_aJ_t^n f(t) = \frac{1}{n!}\int_a^t (t-s)^{n-1} f(s)ds. $$

This is useful in finding analogous expressions for the integral of $f$ when $n$ is not an integer. So, the Riemann-Liouville fractional integral of $f$ of order $\zeta > 0$, where $\zeta \in \mathbb{R}^+$ is given by [2]:

$$ {}_aJ_t^\zeta f(t) = \frac{1}{\Gamma(\zeta)}\int_a^t (t-s)^{\zeta-1} f(s)ds. $$

for $t > a$, where $\Gamma(\zeta)$ is the Gamma function evaluated at $\zeta$. The fractional derivative of $f$ of order $\zeta$ is based upon the Riemann-Liouville integral definition, making fractional derivatives a non-local property. This non-local property is particularly advantageous, providing more accurate numerical solutions for phenomena that fractional differential equations can model [3, 4]. Denoting $n = \lfloor \zeta$ to be

the greatest integer closest to $\zeta$, the Riemann-Liouville fractional derivative is given by:

$$\frac{d^{\zeta} f(t)}{dt^{\zeta}} = \frac{d^n}{dt^n}\left({}_aJ_t^{n-\zeta} f(t)\right).$$

Other commonly used definitions of the fractional derivative include the Caputo-fractional derivative [5], which is given by:

$${}_0^C D_t^{\zeta} f(t) = \frac{1}{\Gamma(n-\zeta)} \int_0^t \frac{f^{(n)}(s)}{(t-s)^{\zeta+1-n}} ds.$$

Differential equations involving derivatives of rational orders can be defined, and most series solutions to these equations are obtained by applying Laplace and inverse Laplace transforms [1]. Due to the non-linear nature of our model, numerical techniques of approximating the solutions prove to be of more excellent utility than analytical solutions. Various methods, such as the fractional Euler method [6] and the generalized Runge-Kutta scheme, have been proposed [7]. Still, we shall use the Adams-Bashforth-Moulton predictor-corrector method, which gives an elegant way of iteratively solving a fractional differential equation subject to the initial conditions [8].

As this method is iterative, we work with a uniform grid having increment step $h$, which may be chosen as $h = T/N$, where $T$ is the time span and $N$ is a natural number. We compute the value of the differential equation at step $t_{n+1}$, assuming the value at $t_n$ is known [2].

In the ordinary first-order differential equation, $Dy(t) = f(t, y(t))$ subject to $y(0) = y_0$, the classical one-step method gives the solution as follows:

$$y(t_{n+1}) = y(t_n) + \int_{t_n}^{t_{n+1}} f(z, y(z)) dz.$$

To compute this integral, we apply the trapezoidal rule, which gives [9, 10]:

$$y(t_{n+1}) = y(t_n) + \frac{h}{2}(f(t_n, y(t_n)) + f(t_{n+1}, y(t_{n+1}))).$$

However, the term on the right-hand side includes the values at $t_{n+1}$, which is unknown to us. In this case, we predict the value, $y^*(t_{n+1})$, which is obtained by the rectangle rule as:

$$y^*(t_{n+1}) = y(t_n) + hy(t_n, y_{t_n}).$$

So, the one-step method may be summarized as:

$$y(t_{n+1}) = y(t_n) + \frac{h}{2}(f(t_n, y(t_n)) + f(t_{n+1}, y^*(t_{n+1}))).$$

We define an analogous scheme in the fractional setup. Let the fractional differential equation of order $\zeta \in \mathbb{R}^+$ be given by [11]:

$$D^{\zeta} y(t) = f(t, y(t)),$$

subject to $y(t_0) = y_0$. The solution to this differential equation is given by the Volterra-integral equation, which may be represented as:

$$y(t) = y(0) + \frac{1}{\Gamma(\zeta)} \int_0^t (t-s)^{\zeta-1} f(s, y(s)) ds.$$

Notice here that the integration starts from 0 to $t$ due to the non-local nature of the fractional derivative. So, the iterative step translates the Volterra equation into [11]:

$$y(t_{n+1}) = y(0) + \frac{1}{\Gamma(\zeta)} \int_0^{t_{n+1}} (t_{n+1}-z)^{\zeta-1} f(z, y(z)) dz.$$

To compute this integral, we make the following approximation:

$$\int_0^{t_{n+1}} (t_{n+1}-z)^{\zeta-1} f(z, y(z)) dz = \frac{h^\zeta}{\zeta(\zeta+1)} \sum_{j=0}^{n+1} a_{j,n+1} f(t_j, y(t_j)),$$

where $a_{j,n+1}$ is a weight function given by:

$$a_{j,n+1} = \begin{cases} n^{\zeta+1} - (n-\zeta)(n+1)^\zeta & j = 0 \\ (n-j+2)^{\zeta+1} + (n-j)^{\zeta+1} - 2(n-j+1)^{\zeta+1} & 1 \le j \le n \\ 1 & j = n+1 \end{cases}$$

So, the analogous predictor-corrector method can be obtained by solving the approximation using the weight functions and putting it into the Volterra equation. This gives:

$$y(t_{n+1}) = y(0) + \frac{h^\zeta}{\Gamma(\zeta)} \left[ f(t_{n+1}, y^*(t_{n+1})) + \sum_{j=0}^{n+1} a_{j,n+1} f(t_j, y(t_j)) \right].$$

To approximate the predicted value, we use the rectangle rule of integration and add suitable weights $b_{j,n+1}$, which gives:

$$y^*(t_{n+1}) = y(0) + \frac{1}{\Gamma(\zeta)} \sum_{j=0}^{n+1} b_{j,n+1} f(t_j, y(t_j)),$$

where $b_{j,n+1} = \frac{h^\zeta}{\zeta}((n+1-j)^\zeta - (n-j)^\zeta)$.

Hence, the Adams-Moulton predictor-corrector method for fractional derivatives can be summarized as:

$$\begin{aligned} y(t_{n+1}) = y(0) + \\ \frac{h^\zeta}{\Gamma(\zeta)} \Bigg[ f\left( t_{n+1}, y(0) + \frac{1}{\Gamma(\zeta)} \sum_{j=0}^{n+1} b_{j,n+1} f(t_j, y(t_j)) \right) \\ + \sum_{j=0}^{n+1} a_{j,n+1} f(t_j, y(t_j)) \Bigg]. \end{aligned} \tag{S1.1}$$

We conducted a comprehensive scenario analysis to evaluate how the exclusion of public health preferences in the payoff structure influences the disclosure behaviour of individuals within a

population (see Figures S1 and S2). Additionally, we explored the impact of varying the fractional-order derivatives in the underlying dynamical system. By comparing these fractional-order models with traditional ordinary differential equation (ODE) models, we observed notable differences in the resulting disease burden across the population (see Figure S3).

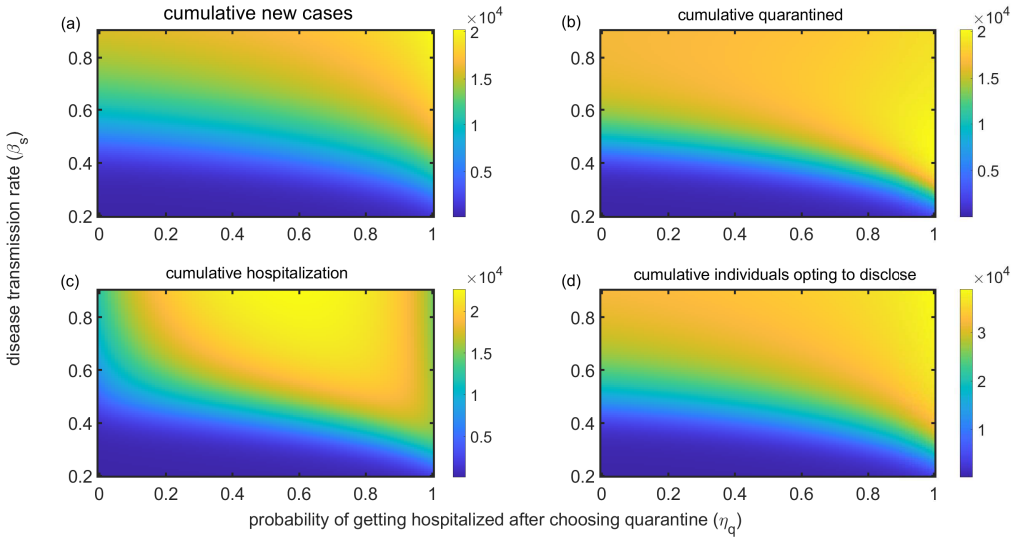


**Figure S1.** Figure represents the (a) cumulative infection (b) cumulative quarantined (c) cumulative hospitalized (d) cumulative quarantined population per day; as a function of the probability of getting hospitals after choosing quarantine ($\eta_q$) and transmission rate ($\beta_s$) without $(1-\eta_q)$ in $p_d$.

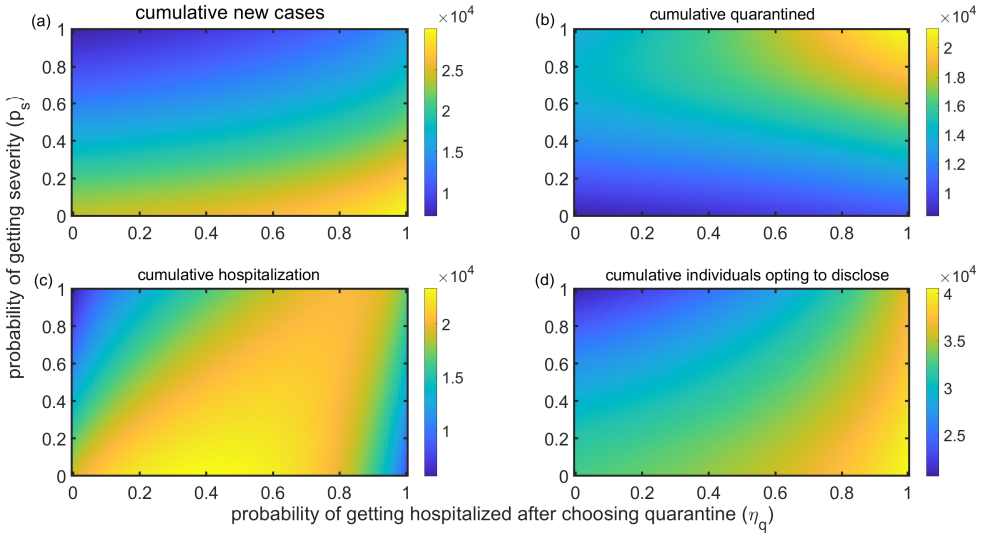


**Figure S2.** Figure represents the (a) cumulative infection (b) cumulative quarantined (c) cumulative hospitalized (d) cumulative quarantined population per day; as a function of preference by public health authorities to provide treatment facility ($\eta_q$) and probability of getting severity ($p_s$) without $(1-\eta_q)$ in $p_d$.

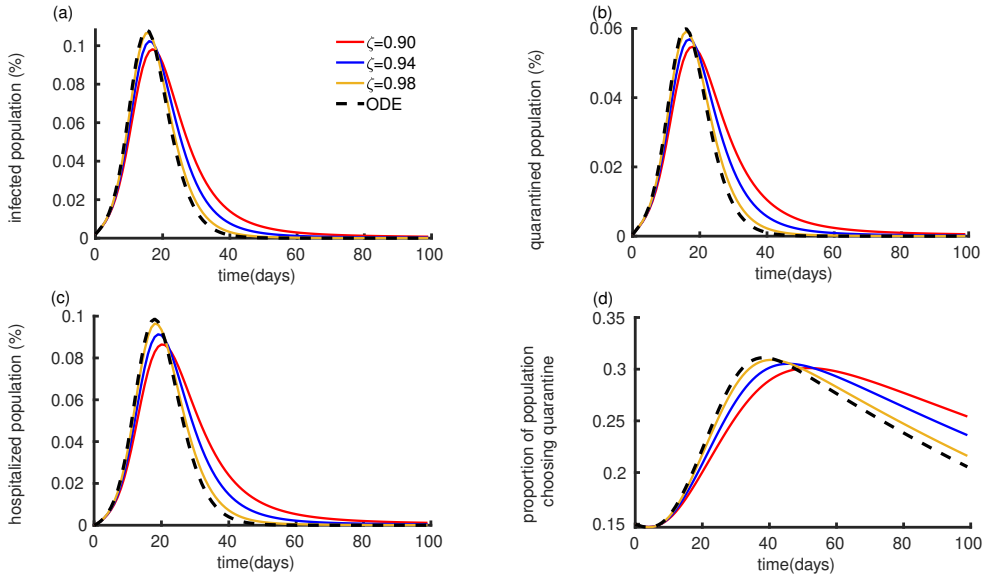


**Figure S3.** Figure represents the time series of (a) infection (%) (b) quarantined (%) (c) hospitalized (%) (d) proportions of the population choosing quarantine per day; for different values of fractional order ($\zeta$) values and ODE model.

## S2. Model implementation, parameter estimation with hospitalization data and interpretation

We analyzed the daily hospitalization data during the pre-vaccine COVID-19 period in Chile and optimized our differential-equation model to this data set. Firstly, we consider the initial 90 data points $y_1, \ldots, y_{90}$, which correspond to a rise and a subsequent peak in daily hospitalizations. The first 90 data points were selected to train the model on a smaller subset of the data, allowing it to evolve and naturally predict the subsequent trend. Based on the parameter spaces $\Theta_e$ and $\Theta_f$, the predictor-corrector algorithm generates a solution curve for the hospitalized population. Denoting the solution curve as the predicted data points $\hat{y_1}, \ldots, \hat{y_{90}}$, we then calculated the cost function given by the sum of squares of the residuals:

$$C = \sum_{i=1}^{90} (y_i - \hat{y_i})^2.$$

To estimate the parameter space $\Theta_e$, we applied the method of least squares to minimize the cost function $C$. The Nelder-Mead optimization method was implemented in Python, and iterative generation of solution curves minimized the cost function based on an initial guess value for $\Theta_f$. The optimization method searches for global optimum values of the parameters in large, specified bounds till a certain tolerance level is reached. Since the Nelder-Mead method is sensitive to the initial guess, we provided generalized guesses and refined them for each parameter to obtain the best likelihood. Similarly, the parameter values in $\Theta_f$ were selected after the model was trained multiple times to give the best fit. We further assumed that the observed new hospitalizations generated from the solution curves followed a randomized Poisson process, whose mean of model-predicted hospitalizations was proportional to the average reporting probability.

## S3. Comparison of Fractional order derivative and the Ordinary differential equation model

The Fractional-order derivative (FOD) has a greater advantage over the Ordinary derivative (OD) in several aspects. Two of the most important aspects are the global nature of the FOD [12], as against the local nature of the OD, and the advantageous memory power that FODs have [12]. This memory power entails the dependency of a system's value at a particular point, not only on the values of points in a local neighbourhood around it, but also on points far from it. More precisely,

**Theorem 1.** *Let $I \subset \mathbb{R}$ be an interval with $0 \in I$. Let $f : I \to \mathbb{R}$ be Riemann integrable. Assume that $0 \in I$ is the base point of integration. For $t_1, t_2 \in I$ with $0 < t_1 < t_2$ and $\zeta \in \mathbb{R}_+$, the difference $J^\zeta f(t_2) - J^\zeta f(t_1)$ is the sum of two terms, one of which is non-zero and which vanishes precisely when $\zeta = 1$.*

*Proof.* Let $X = J^\zeta f(t_2) - J^\zeta f(t_1)$. Definition 2.1 gives us that

$$X = \frac{1}{\Gamma(\zeta)} \int_0^{t_2} (t_2 - t)^{\zeta-1} f(t)\, dt - \frac{1}{\Gamma(\zeta)} \int_0^{t_1} (t_1 - t)^{\zeta-1} f(t)\, dt.$$

A rearrangement of the intervals of integration in this expression yields

$$X = \frac{1}{\Gamma(\zeta)} \left( \int_{t_1}^{t_2} (t_2 - t)^{\zeta-1} f(t)\, dt + \int_0^{t_1} \left( (t_2 - t)^{\zeta-1} - (t_1 - t)^{\zeta-1} \right) f(t)\, dt \right).$$

The required extra term is $\int_0^{t_1} \left( (t_2 - t)^{\zeta-1} - (t_1 - t)^{\zeta-1} \right) f(t)\, dt$, which vanishes at precisely $\zeta = 1$, the ordinary derivative case. □

Hence, in an iterative process, the succeeding approximation will depend on values before $t_1$ and is not restricted to the interval $[t_1, t_2]$ as given by this term. This is particularly useful in numerical techniques, and better approximations of data are expected in the fractional-order case. In many mathematical modelling systems, it becomes necessary to consider the system's state from time $\mathbb{0}$ up to the point whose value is of interest. In such situations, FODs provide elegant properties that allow this incorporation. As an example of data fitting, FODs can potentially provide a higher accuracy than ODE's, as seen in Figure S4. While the qualitative behaviour of both curves is essentially the same regarding the time required to reach the peak, a significant change can be seen in the peak number of hospitalizations. A better knowledge of this is very important for hospital bed allocation, preparedness and dynamic planning by healthcare systems in the face of increasing infection load. We used the same COVID-19 data sets from Chile, South America, to estimate the parameters for the ODE model. We estimated the values of the set of optimized parameters considering the same values of non-optimized parameters that we have chosen for the fractional order derivative model. The values of the optimized and non-optimized parameters are presented in Tables S1 and S2, respectively.

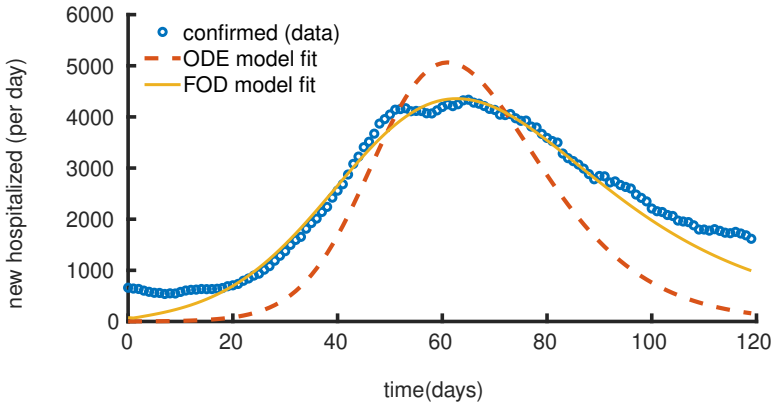


**Figure S4.** Figure represents the dynamics of the Ordinary differential equation (ODE), and the Fractional-order derivative (FOD) model that fits the confirmed new daily hospitalized cases in Chile, South America, for the period from April to September 2020.

**Table S1.** Estimated parameters value with ODE fit.

| Optimized values | Parameters | Description |
|---|---|---|
| $\beta_s$ | Mean disease transmission rate (per day) | 0.3061 |
| $\beta_e$ | Mean incubation rate (per day) | 0.3725 |
| $\eta_q$ | Public health preference of providing treatment facility | 0.6368 |
| $\kappa$ | Sampling rate in social learning (per day) | 0.42984 |
| $A$ | Half saturation coefficient | 199.3979 |
| $c_d$ | Per unit cost of disclosing infection | 0.07769 |
| $c_{nd}$ | Per unit cost of non-disclosing infection | 0.19399 |
| $p_S$ | Probability of developing severity upon infection | 0.86102 |

**Table S2.** Non-optimized parameters value.

| Parameters | Description | Values (day$^{-1}$) |
|---|---|---|
| $\alpha$ | Rate of hospital admissions | 0.016 |
| $\gamma$ | Recovery rate from infection | 0.1 |
| $\gamma_h$ | Recovery rate of hospitalized patients | 0.067 |
| $\mu_h$ | Mortality rate after hospitalization | 0.011 |

## S4. Parameter Sensitivity Analysis

To assess our model's robustness and identify the most influential parameters driving the epidemic dynamics, we conducted a sensitivity analysis using Latin Hypercube Sampling (LHS) with 10,000 samples and a ±5% variation around the optimized parameter values. We computed the Partial Rank Correlation Coefficients (PRCCs) and the corresponding p-values for each parameter. The key results

are summarized in Table S3.

**Table S3.** PRCC values and p-values for the optimized parameters, based on 10,000 samples with a ±5% variation using LHS

| Parameter | PRCC | p-value |
|---|---|---|
| $b_s$ | 0.996243 | $0.000000 \times 10^{+00}$ |
| $b_e$ | 0.912135 | $0.000000 \times 10^{+00}$ |
| $\eta_q$ | 0.404803 | $9.94 \times 10^{-80}$ |
| $\zeta$ | 0.398173 | $5.73 \times 10^{-77}$ |
| $\omega$ | –0.912139 | $0.000000 \times 10^{+00}$ |
| $K$ | 0.310759 | $4.96 \times 10^{-46}$ |
| $c_d$ | 0.107543 | $1.43 \times 10^{-06}$ |
| $c_{nd}$ | –0.916968 | $0.000000 \times 10^{+00}$ |
| $p_s$ | –0.918738 | $0.000000 \times 10^{+00}$ |

## References


1. A. Ali, M. Y. Khan, M. Sinan, F. M. Allehiany, E. E. Mahmoud, A. Abdel-Aty et al., Theoretical and numerical analysis of novel COVID-19 via fractional order mathematical model, *Results Phys.*, **20** (2021), 103676. https://doi.org/10.1016/j.rinp.2020.103676
2. K. Diethelm, N. J. Ford, Analysis of fractional differential equations, *J. Math. Anal. Appl.*, **265** (2002), 229–248. https://doi.org/10.1006/jmaa.2000.7194
3. D. Baleanu, K. Diethelm, E. Scalas, J. J. Trujillo, *Fractional Calculus: Models And Numerical Methods*, World Scientific, 2012.
4. C. Ionescu, A. Lopes, D. Copot, J. A. T. Machado, J. H. T. Bates, The role of fractional calculus in modeling biological phenomena: A review, *Commun. Nonlinear Sci. Numer. Simul.*, **51** (2017), 141–159. https://doi.org/10.1016/j.cnsns.2017.04.001
5. Z. Zheng, W. Zhao, H. Dai, A new definition of fractional derivative, *Int. J. Non-Linear Mech.*, **108** (2019), 1–6. https://doi.org/10.1016/j.ijnonlinmec.2018.10.001
6. K. Shah, A. Ali, S. Zeb, A. Khan, M. A. Alqudah, T. Abdeljawad, Study of fractional order dynamics of nonlinear mathematical model, *Alexandria Eng. J.*, **61** (2022), 11211–11224. https://doi.org/10.1016/j.aej.2022.04.039 .
7. A. Zeb, M. Khan, G. Zaman, S. Momani, V. S. Ertürk, Comparison of numerical methods of the SEIR epidemic model of fractional order, *Z. Naturforsch. A*, **69** (2014), 81–89. https://doi.org/10.5560/ZNA.2013-0073
8. F. A. Rihan. Dynamics of salmonella infection, in *Current Topics in Salmonella and Salmonellosis*, (2017), 151–167. https://doi.org/10.5772/67284
9. N. Hamdan, A. Kilicman, A fractional order SIR epidemic model for dengue transmission, *Chaos Solitons Fractals*, **114** (2018), 55–62. https://doi.org/10.1016/j.chaos.2018.06.031

10. A. Keimer, L. Pflug, Modeling infectious diseases using integro-differential equations: Optimal control strategies for policy decisions and applications in COVID-19, *Res. Gate*, **10** (2020). https://doi.org/10.13140/RG.2.2.10845.44000

11. K. Diethelm, N. J. Ford, A. D. Freed, A predictor-corrector approach for the numerical solution of fractional differential equations, *Nonlinear Dyn.* **29** (2002), 3–22. https://doi.org/10.1023/A:1016592219341

12. K. Diethelm, N. J. Ford, Analysis of fractional differential equations, *J. Math. Anal. Appl.*, **265** (2002), 229–248. https://doi.org/10.1006/jmaa.2000.7194


AIMS Press